

## Accepted Manuscript

Title: Efficient catalytic transfer hydrogenation of biomass-based furfural to furfuryl alcohol with recyclable Hf-phenylphosphonate nano-hybrids

Authors: Hu Li, Yan Li, Zhen Fang, Richard L. Smith Jr.



PII: S0920-5861(18)30517-0  
DOI: <https://doi.org/10.1016/j.cattod.2018.04.056>  
Reference: CATTOD 11412

To appear in: *Catalysis Today*

Received date: 10-12-2017  
Revised date: 10-3-2018  
Accepted date: 24-4-2018

Please cite this article as: Li H, Li Y, Fang Z, Smith RL, Efficient catalytic transfer hydrogenation of biomass-based furfural to furfuryl alcohol with recyclable Hf-phenylphosphonate nano-hybrids, *Catalysis Today* (2018), <https://doi.org/10.1016/j.cattod.2018.04.056>

This is a PDF file of an unedited manuscript that has been accepted for publication. As a service to our customers we are providing this early version of the manuscript. The manuscript will undergo copyediting, typesetting, and review of the resulting proof before it is published in its final form. Please note that during the production process errors may be discovered which could affect the content, and all legal disclaimers that apply to the journal pertain.

# Efficient catalytic transfer hydrogenation of biomass-based furfural to furfuryl alcohol with recycable Hf-phenylphosphonate nanohybrids

Hu Li<sup>1,2,3</sup>, Yan Li<sup>2</sup>, Zhen Fang<sup>1\*</sup>, Richard L. Smith Jr.<sup>3</sup>

<sup>1</sup> Biomass Group, College of Engineering, Nanjing Agricultural University, 40 Dianjiangtai Road, Nanjing, Jiangsu 210031, China

<sup>2</sup> State-Local Joint Engineering Laboratory for Comprehensive Utilization of Biomass, Center for R&D of Fine Chemicals, Guizhou University, Guiyang 550025, China

<sup>3</sup> Tohoku University, Research Center of Supercritical Fluid Technology, Graduate School of Environmental Studies, Aramaki Aza Aoba 6-6-11, Aoba-ku, Sendai 980 8579, Japan

\*Author for correspondence

Zhen Fang (zhenfang@njau.edu.cn)

Web: <http://biomass-group.njau.edu.cn/>

Other emails: Hu Li (huli\_0414@126.com)

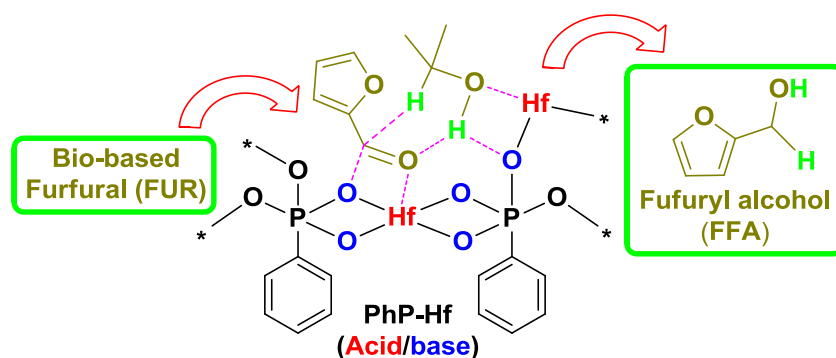
Yan Li (1246613573@qq.com)

Richard L. Smith Jr. (smith@scf.che.tohoku.ac.jp)

Revised submission for a special issue of *Catalysis Today*

March 2018

**Graphic Abstract:**



Mesoporous PhP-Hf(1:1.5) nanohybrid material bearing acidic and basic sites promotes catalytic transfer hydrogenation of furfural to fufuryl alcohol with 97.6% yields with 2-propanol as solvent and hydrogen donor source at 120 °C in 2 h reaction time.

### Highlights:

- Solvothermal method used to prepare mesoporous PhP-Hf(1:1.5) nanohybrid
- Yields of 97.6% fufuryl alcohol obtained from furfural with hybrid material
- Acid-base sites of hybrid material exhibit synergism
- Density and strength of acid-base sites in hybrid material affect activity
- PhP-Hf (1:1.5) recyclable with little change in activity or morphology

### ABSTRACT

An acid-base bifunctional nanohybrid phenylphosphonic acid (PhP) – hafnium (1:1.5) was synthesized through assembly of PhP with HfCl<sub>4</sub> for catalytic transfer hydrogenation of furfural (FUR) to fufuryl alcohol (FFA) using 2-propanol as both reaction solvent and hydrogen donor source. An FFA yield of 97.6% with formation rate of 9760 μmol g<sup>-1</sup> h<sup>-1</sup> at 99.2% FUR conversion was obtained with the reaction

system at 120 °C for 2 h reaction time. Activation energy ( $E_a$ ) was estimated to be 60.8 kJ/mol with respect to FUR concentration, which is comparable with or even lower than  $E_a$  values attained over metal catalysts. The pronounced catalytic activity of PhP-Hf (1:1.5) is attributed to its moderate acidity and relatively strong basicity. The PhP-Hf (1:1.5) catalyst was demonstrated to maintain its activity for five consecutive reuse cycles.

**Keywords:** heterogeneous catalysis; biomass conversion; furfural; acid-base catalysis; transfer hydrogenation

## 1. Introduction

Lignocellulosic biomass is the most abundant organic carbon source in the nature. Many efforts are being made to transform lignocellulosic biomass into biofuels and chemicals with catalytic processes for replacement of petroleum processes [1-3]. Among the catalytic processes, emphasis is being made for upgrading furanic compounds such as furfural (FUR) and 5-hydroxymethylfurfural (HMF) via hydrogenation, oxidation, alkoxylation and rehydration [4-8]. In particular, increasing the hydrogen content in oxygenates using H-donor sources is one of crucial steps for producing energy-intensive molecules efficiently and safely [9-12]. Noble metals (e.g., Au, Pd and Pt) are typically used as catalysts to obtain sufficient yields of target products [13-17]. Nevertheless, the development of low-cost solid functional materials active for catalytic hydrogenation of biomass-based chemicals is required to relieve the demand for noble metals.

One of the most important components in bio-oil, FUR, can be obtained via dehydration of carbohydrates, especially xylose, in the presence of an acid catalyst [18]. This approach, however, is susceptible to humin formation or to the formation of soluble polymers via condensation of the reactive aldehyde group with alcohols, carbonyl and phenolic compounds at high temperatures (> 300 °C) even without a

catalyst [19]. Catalytic hydrogenation of C=O to C–OH can be used to avoid the occurrence of unwanted side reactions [19] and may also enrich transformation routes for FUR upgrading [20]. A number of metallic catalysts (e.g., Pd, Ir, Pt and Ru) have been reported to be efficient for partial hydrogenation of the aldehyde group in FUR, selectively producing furfuryl alcohol (FFA) in yields as high as 98% [21-25]. However, it would be desirable to have non-noble metal (e.g., Cu, Co and Ni) [26-30], with solid materials such as zirconia [31,32], hydrotalcite [33-35], hydroxyapatite [36], and zeolites [37-40] as heterogeneous catalysts for biomass transformations, since these materials are widely available and can contribute to sustainable development .

Trivalent and tetravalent metal organophosphonates are highly insoluble and stable in neutral and acidic reaction media [41,42]. In the present study, a series of hafnium phenylphosphonates (PhP-Hf) were prepared by solvothermal assembly of phenylphosphonic acid (PhP) with HfCl<sub>4</sub> in different P/Hf molar ratios (1:2-2:1) that were characterized to be nanosized and mesoporous with irregular interlayer spacings, as well as having moderate acidity and basicity. Especially, the nanohybrid PhP-Hf(1:1.5) was found to exhibit pronounced catalytic performance in the transfer hydrogenation of FUR to FFA under relatively mild conditions. Reaction conditions were optimized to understand structure-activity relationships, reaction mechanism and reusability of the catalyst.

## 2. Experimental

### 2.1. Materials

Furfural (FUR, >99.5%), furfuryl alcohol (FFA, >98%), phenylphosphonic acid (PhP, ≥98%), HfCl<sub>4</sub> (≥99.9%), HfO<sub>2</sub> (99.9%), SiO<sub>2</sub> (>99.8%), NiO (99.9%), MgO (99.9%), CaO (99.9%), Al<sub>2</sub>O<sub>3</sub> (99.9%), ZrO<sub>2</sub> (99.9%), dimethyl formamide (DMF, 99.8%), naphthalene (≥99.7%), methanol (≥99.9%), ethanol (≥99.5%) and 2-propanol (99.5%) were purchased from Aladdin Industrial Inc. (Shanghai). Other

general-purpose chemicals were purchased from chemical companies and employed without further treatment, unless otherwise noted.

## **2.2. Preparation of Hf-phenylphosphonate hybrids**

Hf-phenylphosphonate (PhP-Hf) hybrids with various P/Zr ratios were prepared by a solvothermal method using different moles of phenylphosphonic acid (PhP) and  $\text{HfCl}_4$  as starting materials. In the general procedure, 316.2 mg PhP (2 mmol) was initially added into a Teflon test tube (100 mL) containing 80 mL DMF, which was stirred (500 rpm) and allowed to be completely dissolved before addition of 906.9 mg  $\text{HfCl}_4$  (3 mmol). Upon stirring for another 20 min, the Teflon tube was transferred into a stainless steel autoclave and sealed, which was then placed into a muffle furnace and statically heated at 120 °C for 24 h. The resulting precipitate was separated by filtration, followed by successively washing with DMF (30 mL  $\times$  3), methanol (25 mL  $\times$  2) and ethanol (20 mL  $\times$  3) to remove the unreacted precursors and residual DMF solvent inside pores, and then dried under vacuum at 80 °C for 8 h. The obtained Hf-phenylphosphonate hybrid was denoted as PhP-Hf (1:1.5), where the values in brackets represent the molar ratio of P to Hf. Other Hf-phenylphosphonate hybrids with different P/Hf molar ratios of 1:2, 1:1, 1.5:1 and 2:1 were prepared and are designated as PhP-Hf (1:2), PhP-Hf (1:1), PhP-Hf (1.5:1) and PhP-Hf (2:1), respectively.

## **2.3. Catalyst characterization**

Fourier transform infrared (FT-IR) spectra were recorded on a Perkin-Elmer 1710 spectrometer (KBr disks). Content of Hf and P species were determined by inductively coupled plasma-optical emission spectrometer (ICP-OES) on a PerkinElmer Optima 5300 DV. X-ray diffraction (XRD) patterns were recorded on a D/max-TTR III X-ray powder diffractometer (radiation source: Cu  $K\alpha$ ). Sample images were obtained with a transmission electron microscope [(HR)-TEM; JEM-1200EX]. Particle size distribution based on about 100 particles was estimated with software (Nano Measurer 1.2, Visual Basic 6.0). Scanning transmission electron

microscope and high-angle annular dark-field (STEM-HAADF) mappings were acquired with an aberration corrected FEI Tecnai G2 F30 S-Twin (S)TEM operating at 300 kV, fitted with energy dispersive X-ray (EDX) spectrometer. Brunauer-Emmett-Teller (BET) surface area, pore size and volume were determined from N<sub>2</sub> physisorption measurements at liquid N<sub>2</sub> temperature on a Micromeritics ASAP 2020 instrument. Thermogravimetry (TG) analyses were carried out on a NETZSCHSTA 429 instrument under an N<sub>2</sub> atmosphere for a programmed-temperature range of 50-600 °C (heating ramp: 10 °C/min). X-ray photoelectron spectroscopy (XPS) measurements were recorded on a Physical Electronics Quantum 2000 Scanning ESCA Microprobe (Al K $\alpha$  anode). Amount of basic and acidic sites in the materials were determined by CO<sub>2</sub>-temperature and NH<sub>3</sub>-temperature programmed desorption (TPD), respectively, using a Micromeritics AutoChem 2920 chemisorption analyzer. In detail, solid samples placed in a quartz reactor were initially degassed at 150 °C for 60 min under a flow of He (50 mL min<sup>-1</sup>). Subsequently, samples were allowed cool via natural convection to 50 °C, and then the treated samples were flushed with 10% CO<sub>2</sub> or NH<sub>3</sub> in He (60 mL min<sup>-1</sup>) for 1 h, followed by purging with pure He (60 mL min<sup>-1</sup>) for the same period. Then, desorption of CO<sub>2</sub> or NH<sub>3</sub> was recorded by a thermal conductivity detector (TCD) at one-second intervals for a programmed temperature range of 50-300 °C (10 °C min<sup>-1</sup>) under He (50 mL min<sup>-1</sup>), and with a hold temperature of 300 °C for 60 min.

#### ***2.4. Typical reaction procedure for conversion of FUR to FFA***

All reactions were carried out in Ace borosilicate glass pressure test tubes (15 mL) in an oil bath. Typically, 1.0 mmol FUR, 5 mL 2-propanol, and 0.05 g catalyst were added into the test tube, and placed into an oil bath that was pre-heated to a set temperature of 80-140 °C. The reaction mixture was magnetically stirred at 600 rpm for a specific reaction time of 0.25-10 h. After a given reaction time, the test tube was cooled down to room temperature with water in a beaker. The resulting liquid samples were collected with an injector and passed through a filter membrane (pore size: 0.22  $\mu$ m) prior to quantitative analysis by gas chromatography (GC).

Liquid samples were identified by GC-MS (Agilent 6890N GC / 5973 MS). FUR, FFA and byproducts (e.g., furfural diisopropyl acetal, 2-isopropoxymethylfuran, and isopropyl levulinate) were analyzed with GC (Agilent 7890B) using a HP-5 column (30 m  $\times$  0.320 mm  $\times$  0.25  $\mu$ m) equipped with a flame ionization detector (FID) by addition of naphthalene (ca. 20 mg) as internal standard. The conversion of FUR and FFA yields were calculated on the basis of standardized curves with five points made from commercial samples.

After each reaction, the solid residue in the solution was separated by centrifugation (12000 rpm) for 3 min, followed by successively washing with ethanol (25 mL  $\times$  3) and acetone (20 mL  $\times$  2) under ultrasonic treatment, and drying at 80  $^{\circ}$ C for 6 h. The obtained catalyst was directly used for the next run. To examine leaching of the Hf and P species, ICP analyses of the supernatant liquids that were volumetrically diluted with water were performed.

### 3. Results and discussion

#### 3.1. Catalyst characterization

Structural functionalities of the prepared PhP-Hf (1:1.5) hybrid and commercial HfO<sub>2</sub> were initially examined with FT-IR (Fig. 1). Both PhP-Hf (1:1.5) and HfO<sub>2</sub> had a wide stretching region of 3200-3600 cm<sup>-1</sup> and bending vibration at 1640 cm<sup>-1</sup>, which can be ascribed to the presence of -OH species and water molecules, respectively [43]. The partially overlapping band near 1600 cm<sup>-1</sup> belongs to phenyl group stretching, while the bands at 1485 and 1435, and 3000 cm<sup>-1</sup> are assigned to the skeletal vibration and C-H stretching vibration of the aromatic ring, respectively [44]. It should be noted that the bands around 2770 and 2400cm<sup>-1</sup> are possibly due to the stretching vibration of O-H species in monohydrogen phosphonate groups [45]. Bands at around 560 and 760, 695 and 750, 900-1120, and 1165 cm<sup>-1</sup> are characteristic of Hf-O bonds, monosubstituted phenyl ring vibrations, asymmetric and symmetric P-O stretching

vibrations of tetrahedral C-PO<sub>3</sub> groups, and P-C stretching vibration, respectively [46]. Although the characteristic band at 760 cm<sup>-1</sup> of Hf-O bond in PhP-Hf (1:1.5) was partially overlapped with that of the phenyl ring vibration (750 cm<sup>-1</sup>), the distinct blueshift of the band from 520 cm<sup>-1</sup> for HfO<sub>2</sub> to 560 cm<sup>-1</sup> for PhP-Hf (1:1.5) showed that a relationship existed between Hf-O with P species.

<Fig. 1>

XRD patterns of HfO<sub>2</sub> showed that the material was crystalline and mixed with tetragonal (t) and monoclinic (m) structures, while PhP-Hf (1:1.5) had an amorphous structure (Fig. 1B). Notably, an additional reflection with *d*-spacing of 14.9 Å at 2θ of 5.9° was observed in the case of PhP-Hf (1:1.5), which was most likely due to the interlayer distance of Hf layers being held apart by PhP [47]. Correspondingly, nitrogen adsorption-desorption isotherms (Fig. 1C) gave H1-type and H4-type loops for HfO<sub>2</sub> and PhP-Hf(1:1.5), respectively, illustrating an increase in BET surface area (214 m<sup>2</sup>/g) and pore volume (0.21 cm<sup>3</sup>/g) but a decrease in average pore size (3.4 nm) of PhP-Hf (1:1.5), as compared with those of HfO<sub>2</sub> (Table 1). These results substantiated the formation of extra interlayers via assembly that significantly contributed to improving surface texture to have more substrate-accessible active sites. The molar ratio of P/Hf in the PhP-Hf (1:1.5) hybrid was found to be 1.07 (epiphase) by XPS quantitative analysis, which was much higher than that (0.68, bulk phase) obtained by ICP analysis. The difference of P/Hf molar ratio in epiphase and epiphase of PhP-Hf (1:1.5) indicated that the organic ligand (PhP) preferred to be located on the surface of the formed hybrid, while Hf was mainly encapsulated inside the material. The thermal stability of PhP-Hf (1:1.5) and HfO<sub>2</sub> is shown in Fig. 1D. Both PhP-Hf (1:1.5) and HfO<sub>2</sub> were stable up to 300 °C, so that weight loss in the temperature range of 300-550 °C can be attributed to removal of weakly bonded -OH species (Fig. 1A). When samples were brought to temperatures above 550 °C, large weight loss was observed for PhP-Hf (1:1.5) (Fig. 1D), that can be attributed to the decomposition of organic species.

<Table 1>

In view of the PhP-Hf (1:1.5) hybrid being highly stable below 300 °C, its acidic and basic densities were evaluated by NH<sub>3</sub>- and CO<sub>2</sub>-TPD over the temperature-programmed range of 50-300 °C and at a maximum holding temperature of 300 °C (Table 1). Basic (0.32 mmol/g) and acidic (0.27 mmol/g) content of PhP-Hf (1:1.5) was observed to be relatively higher than that of HfO<sub>2</sub> (Table 1); in particular, a significant increase in the content of acid sites relative to that of basic sites lead to the formation of additional acidic –OH species possibly derived from Zr-OH and P-OH groups [48]. To further elucidate the basic and acidic strength of PhP-Hf (1:1.5) and HfO<sub>2</sub>, XPS analyses were performed (Fig. 2). The binding energies of Hf 4f in PhP-Hf (1:1.5) at 17.4 and 18.9 eV were slightly larger than those (16.9 and 18.5 eV) of Hf 4f in HfO<sub>2</sub>, respectively (Fig. 2A), showing the formation of Hf species in the hybrid with strong Lewis acidity [49]. On the other hand, a relatively higher binding energy of O 1s (531.3 eV) assigned to P-O-Hf interaction in PhP-Hf (1:1.5) than that of Hf(H)-O-Hf interaction in HfO<sub>2</sub> (Fig. 2B) due to the much smaller negative charge on the oxygen species [50,51], which was directly correlated with lower base strength of PhP-Hf (1:1.5) compared with that of HfO<sub>2</sub>. These results showed that the introduction of organic ligand PhP could stabilize the Hf species with respect to both acid content and strength of PhP-Hf (1:1.5) [52], and that the formed P-O-Hf framework in PhP-Hf (1:1.5) with interlayers appeared to increase surface area and pore volume, thus increasing its basic content achieved by its superior accessibility to HfO<sub>2</sub>. The Hf-O-Hf framework or hydroxide species in HfO<sub>2</sub> seemed to give enhanced basic strength in comparison with PhP-Hf (1:1.5).

< Fig. 2 >

HR-TEM images indicated the presence of amorphous and crystalline [tetragonal (t) and monoclinic (m)] structures in PhP-Hf (1:1.5) and HfO<sub>2</sub>, respectively (Fig. 3), which was consistent with XRD analyses (Fig. 1B). Worm-like stripes present in Fig. 3A were most likely the result of disordered interlayers of the PhP-Hf (1:1.5) nanohybrid materials. Moreover, STEM-HAADF images with corresponding

elemental mappings in Fig. 4 demonstrated good spatial arrangement of Hf, C, O and P species in PhP-Hf (1:1.5), showing even dispersion and connection of Hf and C-PO<sub>3</sub> moieties throughout the nanohybrid material. All of these unique physicochemical characteristics make PhP-Hf (1:1.5) a promising material for heterogenous transfer hydrogenations.

<Fig. 3>

<Fig. 4>

### ***3.2. Transfer hydrogenation of FUR to FFA with different catalysts***

Preliminary studies were conducted with different oxides (SiO<sub>2</sub>, NiO, MgO, CaO, Al<sub>2</sub>O<sub>3</sub>, ZrO<sub>2</sub> and HfO<sub>2</sub>), the prepared PhP-Hf (1:1.5) nanohybrid material and the corresponding synthetic precursors (PhP and HfCl<sub>4</sub>) as catalysts for transfer hydrogenation of FUR to FFA using 2-propanol as H-donor source at 120 °C for 2 h (Table 2). Neither weakly acidic oxides (e.g. SiO<sub>2</sub>) nor weakly basic metal oxides (e.g. NiO, MgO and CaO) could efficiently catalyze transfer hydrogenation of FUR (Entries 1-4, Table 2), which is in accordance with literature results for transfer hydrogenation of ethyl levulinate to  $\gamma$ -valerolactone using metal hydroxides [53]. In these catalytic systems, furfural diisopropyl acetal derived from acetalization of FUR with 2-propanol was detected to be the dominant byproduct, particularly in the presence of an acidic catalyst (e.g., SiO<sub>2</sub>) [54]. In sharp contrast, metal oxides bearing both basic and acidic sites were active for FFA synthesis (Entries 5-7, Table 2), wherein basic sites were postulated to assist in the formation of isopropoxide from 2-propanol on acidic sites by proton abstraction, thus giving a six-membered intermediate among acid sites, alcohol and aldehyde groups to transfer  $\beta$ -H and finally yield FFA [55]. The prepared PhP-Hf (1:1.5) nanohybrid material, which had higher strength acidic and lower strength basic sites in comparison with HfO<sub>2</sub> (Table 1), was able to produce FFA in almost quantitative yield (97.6%) and at high formation rate (9760  $\mu\text{mol g}^{-1} \text{h}^{-1}$ ) from FUR at 99.2% conversion (Table 2, entry 8). When a strong base (NaOH) was used as catalyst, FUR was also converted but via Cannizzaro reaction [56], affording mixed products of FFA and 2-furoic acid in nearly same

yields of ca. 21.3% (entry 9). The strong acidic precursors of PhP-Hf (1:1.5) including PhP and HfCl<sub>4</sub> could not selectively catalyze FUR (Entries 10-11, Table 2), while furfural diisopropyl acetal, 2-isopropoxymethylfuran and isopropyl levulinate were found to be the major products under identical reaction conditions. Therefore, the presence of both acid-base sites having appropriate content and strength seemed to be key factors for the selective production of FFA from FUR with the prepared catalytic materials. Compared with PhP-Hf (1:1.5), the lower catalytic activity of PhP-Ni (1:1.5), PhP-Al (1:1.5), and PhP-Zr (1:1.5) (Table 2, Entries 12-14) clearly indicated the unique role that the Hf species have in the formation of acid-base sites that promote transfer hydrogenation. Notably, the obtained FFA selectivity (98.4%) over the prepared PhP-Hf (1:1.5) hybrid (Table 2, Entry 8) is superior to 5 wt% Pd/C (87.1%) and comparable to 5% Pd-5% Cu/MgO (99.0%) at 130 °C under 0.8 MPa H<sub>2</sub> after 100 min and 55 min reaction time, respectively [21].

**<Table 2>**

**3.3. Effect of acidity/basicity on catalytic transfer hydrogenation of FUR to FFA**

To further investigate the influence of both content and strength of acid-base sites on the catalytic transfer hydrogenation of FUR to FFA, a series of PhP-Hf hybrids with different P/Hf molar ratios were prepared (Table 3). XPS analyses showed a slightly higher P/Hf ratio than the actual feed ratio that was supported by ICP analysis, demonstrating that the organic ligand PhP rather than Hf species was prone to be assembled on the hybrid surface in accordance with results in *vide supra*. With an increase in the relative Hf content (Table 3), the reactivity of the corresponding hybrids became greatly enhanced, with a maximum yield (97.6%) and selectivity (98.4%) of FFA with a turnover number (TON) value (33.6) being obtained when the P/Hf ratio was 1:1.5. With a decrease in the P/Hf ratio of 2:1 to 1:2, both acid-base site contents were characterized separately by NH<sub>3</sub>- and CO<sub>2</sub>-TPD and found to steadily increase from 0.44 to 0.65 mmol/g, while acid/base site ratios slightly increased from 0.82 to 0.87 (Fig. 5, Table 3). This indicates that the acid-base content of 0.59 mmol/g with acid/base site ratio of 0.84 in the case of PhP-Hf (1:1.5) is

favorable for the selective production of FFA from FUR. The strength of acidic and basic sites of these PhP-Hf hybrids as given by XPS (Fig. 6) were found to be negatively correlated with the P/Hf ratio (Fig. 6A), while the base strength was initially enhanced with the reduction of the P/Hf ratio from 2:1 to 1:1.5, and then became weak as the P/Hf ratio further decreased to 1:2 (Fig. 6B). Considering the above results, it could be concluded that the catalytic performance of the PhP-Hf (1:1.5) hybrid in the transfer hydrogenation of FUR to FFA (Table 3) could be attributed to its moderate content of acid-base sites and medium acidity and relatively stronger basicity, despite the basicity of the sites being weaker than those of HfO<sub>2</sub> (Fig. 2B).

<Table 3>

<Fig. 5>

<Fig. 6>

A reaction mechanism can be proposed analogous to the catalytic pathway of Meerwein-Ponndorf-Verley reduction [57-59] that considers the synergistic role of acid (Hf<sup>4+</sup>) and base (O<sup>2-</sup>) sites of PhP-Hf (1:1.5) in the transfer hydrogenation of FUR to FFA. A key transition state, which is shown in Fig. 7, is proposed to be formed *in situ* among FUR, 2-propanol, and acid-base coupled species (Hf<sup>4+</sup>-O<sup>2-</sup>). In general, a pair of acid-base sites (Hf<sup>4+</sup>-O<sup>2-</sup>) assists in the adsorption of 2-propanol onto PhP-Hf (1:1.5) and is capable of leading to the generation of isopropoxide and hydride by dissociation. The aldehyde group in FUR is probably activated by acidic Hf<sup>4+</sup> species, thus resulting in the formation of a transition state with six links to fulfill the hydrogen transfer route to yield FFA and acetone (Fig. 7). In the transformation, some side products such as furfural diisopropyl acetal, 2-isopropoxymethylfuran, isopropyl levulinate, and 2-furoic acid may be formed in the presence of relatively stronger acidic and basic sites, respectively (Fig. 7).

<Fig. 7>

### 3.4. Effect of reaction temperature and time on catalytic conversion of FUR to FFA

Typically, reaction rate and product distribution are closely correlated with reaction temperature and time. Table 4 summarizes catalytic results of FUR-to-FFA conversion with PhP-Hf (1:1.5) at 80-140 °C after 0.25-10 h. Both FUR conversion and reaction rates were sensitive to reaction temperature in which the highest TOF value ( $68.5 \text{ h}^{-1}$ ) that could be obtained occurred at 140 °C for 0.25 h reaction time, and more than 90% conversion was obtained in less than 1.5 or 1 h as the reaction took place at relatively high temperatures of 120 or 140 °C. Furfural diisopropyl acetal was observed to be the dominant co-product either at relatively low temperatures (80 and 100 °C) or at short reaction times (0.25-1 h), thus leading to lower yields and selectivities of FFA from FUR. Interestingly, the formed acetal could be reversibly transformed into FUR by prolonging the reaction duration, which was verified by the gradual increase in FFA selectivity (Table 4). Under relatively harsh reaction conditions (e.g., 140 °C for 4 or 6 h), some undesirable products (e.g., furan-based esters, ethers and polymers) in small amounts derived from side reactions such as Cannizzaro and polycondensation were observed [60] that resulted in the decrease of FFA yield and selectivity. The carbon balance for all the reactions was found to be no less than 85%. From the point of view of saving energy, reactions proceeding at moderate conditions (e.g. 120 °C, 2 h reaction time) are most likely to be close to optimal for the catalytic transfer hydrogenation of FUR. Importantly, it was observed that the TOF value of  $16.8 \text{ h}^{-1}$  obtained at 120 °C was superior to those at 80 °C ( $8.2 \text{ h}^{-1}$ ) and 100 °C ( $12.7 \text{ h}^{-1}$ ), and comparable to that ( $16.9 \text{ h}^{-1}$ ) obtained at a higher temperature of 140 °C for the same reaction time of 2 h.

**<Table 4>**

The catalytic hydrogenation of FUR has been reported to be pseudo-first order with respect to FUR concentration [61,62]. At first, the initial reaction rate constants ( $k$ ) of PhP-Hf (1:1.5) at different reaction temperatures of 353, 373 and 393 K were calculated by plotting the values of  $-\ln(1 - X)$  ( $X$  = FUR conversion) against variable reaction times ( $t$ ) in the range of 15 to 120 min (Fig. 8A). From an Arrhenius plot of the data (Fig. 8B), the apparent activation energy ( $E_a$ ) was estimated to be 60.8

kJ/mol, which is comparable to and even lower than previously reported  $E_a$  values using metal catalysts for the same reaction including e.g., supported Ni (QD3): 40-60 kJ/mol [63], ZrPN: 70.5 kJ/mol [49], Cu-Mg-Al: 66 kJ/mol [64], and CuMgAl: 127 kJ/mol [65]. The pronounced catalytic results of PhP-Hf (1:1.5) clearly demonstrates that the prepared materials are highly active for transfer hydrogenation of FUR to FFA.

<Fig. 8>

### **3.5. Effect of catalyst dosage on transfer hydrogenation of FUR to FFA**

The effect of PhP-Hf (1:1.5) dosage on catalytic transfer hydrogenation of FUR to FFA was studied (Table 5). It could be observed that almost no FUR (<1.0%) was converted into FFA in the absence of PhP-Hf (1:1.5), implying that the reaction could not occur spontaneously (Entry 1, Table 5). Once the addition of 12 mg PhP-Hf (1:1.5) (FUR/catalyst mass ratio: 8.0), FFA yield reached 40.7% (TON: 60.2) under identical conditions (Entry 2, Table 5). The catalytic activity regarding the yields of FFA linearly increased by further increasing the catalyst dosage (Entries 2-4, Table 5), and high FFA yields of 97.6% and FUR conversions of 99.2% with moderate TON of 33.6 were obtained using PhP-Hf(1:1.5) at a FUR/catalyst mass ratio of 1.9 (Entry 4, Table 5). Then, both FFA yields and FUR conversions leveled off, giving low TON values (Entries 5-6, Table 5). It should be noted that FFA selectivity showed little change, regardless of the amount of catalyst. In this regard, PhP-Hf (1:1.5) with a dosage of 50 mg (FUR/catalyst mass ratio: 1.9) seems to be a robust candidate for the synthesis of FFA from FUR.

<Table 5>

### **3.6. Catalyst recycle study**

At the above optimized reaction conditions for 50 mg catalyst at 120 °C for 2 h, the recycle of PhP-Hf (1:1.5) in the transfer hydrogenation of FUR to FFA was studied (Fig. 9). As shown in Fig. 10, FFA yields were only slightly reduced from 97.6% to 92.3% at FUR conversions of 93.6-99.2% over PhP-Hf (1:1.5) in five consecutive

reaction cycles. Stable FFA selectivities in the range of 98.3-98.8% were observed during the recycle runs, further indicating the robust acid-base sites in the PhP-Hf (1:1.5) hybrid. ICP analyses showed that less than 1.2 and 1.8 ppm of Hf and P species were leached into the alcoholic solution after the first round of reactions. There was no significant change in textural structure (surface area, pore size and volume) and acid-base properties of PhP-Hf (1:1.5) before and after five cycles of reactions (Table 1). The slight decrease in FFA yield and FUR conversion is probably caused by the partial adsorption of organic species such as isopropoxide derived from 2-propanol, which is supported by the appearance of additional bands at around 2900  $\text{cm}^{-1}$  (Fig. 10) possibly assigned to C-H stretching vibrations of methyl and ethyl groups in isopropoxide, and the reduced intensity that is probably due to the coverage of exogenous organic species of the bands at near 1600  $\text{cm}^{-1}$  belonging to the stretching vibration of phenyl groups in PhP moieties.

<Fig. 9>

<Fig. 10>

## Conclusions

Hybrid PhP-Hf (1:1.5) catalysts that are highly-active for transfer hydrogenation can be prepared by solvothermal treatment of phenylphosphonic acid (PhP) with  $\text{HfCl}_4$  in a molar ratio of 1:1.5 at 120 °C for 24 h treatment time. The PhP-Hf (1:1.5) materials were characterized and found to be nanosized (13.7 nm), mesoporous (average pore size: 3.4 nm), and bifunctionalized with acid (0.27 mmol/g) and base (0.32 mmol/g) sites. The PhP-Hf (1:1.5) nanohybrid was demonstrated to have good catalytic performance in transfer hydrogenation of FUR with 2-propanol, giving FFA in yields of up to 97.6% after reaction for 2 h at 120 °C. The superior catalytic activity with moderate activation energy ( $E_a = 60.8 \text{ kJ/mol}$ ) could be attributed to the moderate acidity and relatively strong basicity of the catalytic sites in the PhP-Hf (1:1.5) nanohybrid materials. In the reaction mechanism, a key transition state forms among FUR, 2-propanol, and acid-base coupled species ( $\text{Hf}^{4+}\text{-O}^{2-}$ ). The PhP-Hf (1:1.5)

nanohybrid catalyst was determined to be recyclable with no distinct loss in activity for at least five reaction cycles.

## Acknowledgments

This work is financially supported by Nanjing Agricultural University (68Q-0603), International Postdoctoral Exchange Fellowship Program of China (20170026), Postdoctoral Science Foundation of China (2016M600422), and Jiangsu Postdoctoral Research Funding Plan (1601029A).

## References

- [1] H. Li, Z. Fang, R. L. Smith, S. Yang, *Prog. Energ. Combust.* 55 (2016) 98-194.
- [2] G. Kumar, S. Shobana, W. H. Chen, Q. V. Bach, S. H. Kim, A. E. Atabani, J. S. Chang, *Green Chem.* 19 (2017) 44-67.
- [3] Z. Fang, R. L. Smith, H. Li, *Production of biofuels and chemicals with bifunctional catalysts*, first ed., Springer, Singapore, 2017.
- [4] J. P. Lange, E. van der Heide, J. van Buijtenen, R. Price, *ChemSusChem* 5 (2012) 150-166.
- [5] H. Li, S. Yang, A. Riisager, A. Pandey, R. S. Sangwan, S. Saravanamurugan, R. Luque, *Green Chem.* 18 (2016) 5701-5735.
- [6] P. Zhou, Z. Zhang, *Catal. Sci. Technol.* 6 (2016) 3694-3712.
- [7] B. Liu, Z. Zhang, *ChemSusChem* 9 (2016) 2015-2036.
- [8] P. N. Paulino, R. F. Perez, N. G. Figueiredo, M. A. Fraga, *Green Chem.* 19 (2017) 3759-3763.
- [9] J. N. Chhed, J. A. Dumesic, *Catal. Today* 123 (2007) 59-70.
- [10] X. Tang, J. Wei, N. Ding, Y. Sun, X. Zeng, L. Hu, S. Liu, T. Lei, L. Lin, *Renew. Sustain. Energ. Rev.* 77 (2017) 287-296.
- [11] M. J. Gilkey, B. Xu, *ACS Catal.* 6 (2016), 1420-1436.
- [12] H. Li, A. Riisager, S. Saravanamurugan, A. Pandey, R. S. Sangwan, S. Yang, R. Luque, *ACS Catal.*, 2018, 8, 148-187.

- [13] Y. Nakagawa, S. Liu, M. Tamura, K. Tomishige, *ChemSusChem* 8 (2015) 1114-1132.
- [14] A. Zuliani, F. Ivars, R. Luque, *ChemCatChem* (2017) DOI: 10.1002/cctc.201701712
- [15] Q. Xia, Z. Chen, Y. Shao, X. Gong, H. Wang, X. Liu, S. F. Parker, X. Han, S. Yang, Y. Wang, *Nat. Commun.* 7 (2016) 11162.
- [16] H. Wang, H. Ruan, H. Pei, H. Wang, X. Chen, M. P. Tucker, J. R. Cort, B. Yang, *Green Chem.* 17 (2015) 5131-5135.
- [17] X. L. Du, L. He, S. Zhao, Y. M. Liu, Y. Cao, H. Y. He, K. N. Fan, *Angew. Chem.* 123 (2011) 7961-7965.
- [18] R. M. López, P. Maireles-Torres, M. Ojeda, I. Sadaba, M. L. Granados, *Energy Environ. Sci.* 9 (2016) 1144-1189.
- [19] C. Wang, Z. Guo, Y. Yang, J. Chang, A. Borgna, *Ind. Eng. Chem. Res.* 53 (2014) 11284-11291.
- [20] K. Yan, G. Wu, T. Lafleur, C. Jarvis, *Renew. Sustain. Energ. Rev.* 38 (2014) 663-676.
- [21] K. Fulajtárova, T. Soták, M. Hronec, I. Vávra, E. Dobročka, M. Omastovác, *Appl. Catal. A: Gen.* 502 (2015) 78-85.
- [22] Y. Nakagawa, K. Takada, M. Tamura, K. Tomishige, *ACS Catal.* 4 (2014) 2718-2726.
- [23] M. J. Taylor, L. J. Durndell, M. A. Isaacs, C. M. A. Parlett, K. Wilson, A. F. Lee, G. Kyriakou, *Appl. Catal. B: Environ.* 180 (2016) 580-585.
- [24] P. Panagiotopoulou, N. Martín, D. G. Vlachos, *ChemSusChem* 8 (2015) 2046-2054.
- [25] Q. Yuan, D. Zhang, L. van Haandel, F. Ye, T. Xue, E. J. Mhensen, Y. Guan, *J. Mol. Catal. A: Chem.* 406 (2015) 58-64.
- [26] C. P. Jiménez-Gómez, J. A. Cecilia, D. Durán-Martín, R. Moreno-Tost, J. Santamaría-González, J. Mérida-Robles, R. Mariscal, P. Maireles-Torres, *J. Catal.* 336 (2016) 107-115.
- [27] B. M. Nagaraj, V. Siva Kumar, V. Shasikala, A. H. Padmasri, B. Sreedhar, B. David Raju, K. S. Rama Rao, *Catal. Commun.* 4 (2003) 287-293.
- [28] X. Chen, H. Li, H. Luo, M. Qiao, *Appl. Catal. A: Gen.* 233 (2002) 13-20.
- [29] B. Liu, L. Lu, B. Wang, T. Cai, K. Iwatani, *Appl. Catal. A: Gen.* 171 (1998) 117-122.
- [30] T. P. Sulmonetti, S. H. Pang, M. T. Claire, S. Lee, D. A. Cullen, P. K. Agrawal, C. W. Jones, *Appl. Catal. A: Gen.* 517 (2016) 187-195.

- [31] N. S. Biradar, A. M. Hengne, S. S. Sakate, R. K. Swami, C. V. Rode, *Catal. Lett.* 146 (2016) 1611-1619.
- [32] V. Montes, J. F. Miñambres, A. N. Khalilov, M. Boutonnet, J. M. Marinas, F. J. Urbano, A. M. Maharramov, A. Marinas, *Catal. Today* (2018) DOI: <https://doi.org/10.1016/j.cattod.2017.05.022>
- [33] K. Yan, Y. Liu, Y. Lu, J. Chai, L. Sun, *Catal. Sci. Technol.* 7 (2017) 1622-1645.
- [34] J. Zhang, J. Chen, *ACS Sustainable Chem. Eng.* 5 (2017) 5982-5993.
- [35] H. Chen, H. Ruan, X. Lu, J. Fu, T. Langrish, X. Lu, *Mol. Catal.* 445 (2018) 94-101.
- [36] F. Wang, Z. Zhang, *ACS Sustainable Chem. Eng.* 5 (2017) 942-947.
- [37] M. Koehle, R. F. Lobo, *Catal. Sci. Technol.* 2016, 6 (2016) 3018-3026.
- [38] Y. Injongkol, T. Maihom, P. T. J. Sirijaraensre, B. Boekfa, J. Limtrakul, *Phys. Chem. Chem. Phys.* 19 (2017) 24042-24048.
- [39] L. Bui, H. Luo, W. R. Gunther, Y. Román-Leshkov, *Angew. Chem. Int. Ed.* 52 (2013) 8022-8025.
- [40] X. Li, P. Jia, T. Wang, *ACS Catal.* 6 (2016) 7621-7640.
- [41] K. J. Gagnon, H. P. Perry, A. Clearfield, *Chem. Rev.* 112 (2012) 1034-1054.
- [42] Y. P. Zhu, T. Z. Ren, Z. Y. Yuan, *Catal. Sci. Technol.* 5 (2015) 4258-4279.
- [43] H. Li, Z. Fang, J. He, S. Yang, *ChemSusChem* 10 (2017) 681-686.
- [44] A. Cabeza, M. A. Aranda, S. Bruque, D. M. Poojary, A. Clearfield, J. Sanz, *Inorg. Chem.* 37 (1998) 4168-4178.
- [45] J. Veliscek-Carolan, T. L. Hanley, V. Luca, *Sep Purif. Technol.* 129 (2014) 150-158.
- [46] A. G. Miguel, *J. Mater. Chem.* 6 (1996) 639-644.
- [47] R. Silbernagel, C. H. Martin, A. Clearfield, *Inorg. Chem.* 55 (2016), 1651-1656.
- [48] F. Li, L. J. France, Z. Cai, Y. Li, S. Liu, H. Lou, J. Long, X. Li, *Appl. Catal. B: Environ.* 214 (2017) 67-77.
- [49] H. Li, J. He, A. Riisager, S. Saravanamurugan, B. Song, S. Yang, *ACS Catal.* 6 (2016) 7722-7727.
- [50] J. Song, B. Zhou, H. Zhou, L. Wu, Q. Meng, Z. Liu, B. Han, *Angew. Chem. Int. Ed.* 54 (2015) 9399-9403.

- [51] B. Tang, W. Dai, X. Sun, G. Wu, N. Guan, M. Hunger, L. Li, *Green Chem.* 17 (2015) 1744-1755.
- [52] C. Xie, J. Song, B. Zhou, J. Hu, Z. Zhang, P. Zhang, Z. Jiang, B. Han, *ACS Sustainable Chem. Eng.* 4 (2016) 6231-6236.
- [53] X. Tang, H. Chen, L. Hu, W. Hao, Y. Sun, X. Zeng, L. Lin, S. Liu, *Appl. Catal. B: Environ.* 147 (2014) 827-834.
- [54] J. M. Rubio-Caballero, S. Saravanamurugan, P. Maireles-Torres, A. Riisager, *Catal. Today* 234 (2014) 233-236.
- [55] T. Komanoya, K. Nakajima, M. Kitano, M. Hara, *J. Phys. Chem. C* 119 (2015) 26540-26546.
- [56] S. Subbiah, S. P. Simeonov, J. M. S. S. Esperança, L. P. N. Rebelo, C. A. M. Afonso, *Green Chem.* 15 (2013) 2849-2853.
- [57] R. S. Assary, L. A. Curtiss, J. A. Dumesic, *ACS Catal.* 3 (2013) 2694-2704.
- [58] A. N. Ajjou, *Catal. Today* 247 (2015) 177-181.
- [59] V. L. Sushkevich, I. I. Ivanova, S. Tolborg, E. Taarning, *J. Catal.* 316 (2014) 121-129.
- [60] M. Choura, N. M. Belgacem, A. Gandini, *Macromolecules* 29 (1996) 3839-3850.
- [61] S. P. Lee, Y. W. Chen, *Ind. Eng. Chem. Res.* 38 (1999) 2548-2556.
- [62] R. V. Sharma, U. Das, R. Sammynaiken, A. K. Dalai, *Appl. Catal. A: Gen.* 454 (2013) 127-136.
- [63] X. Chen, W. Sun, N. Xiao, Y. Yan, S. Liu, *Chem. Eng. J.* 126 (2007) 5-11.
- [64] M. M. Villaverde, T. F. Garetto, A. J. Marchi, *Catal. Commun.* 58 (2015) 6-10.
- [65] M. M. Villaverde, N. M. Bertero, T. F. Garetto, A. J. Marchi, *Catal. Today* 213 (2013) 87-92.

### Table and Figure Captions:

**Table 1.** Textural and acid-base properties of HfO<sub>2</sub> and PhP-Hf (1:1.5)

**Table 2.** Transfer hydrogenation of FUR to FFA with different catalysts

**Table 3.** Effect of different P/Hf ratios on transfer hydrogenation of FUR to FFA

**Table 4.** Effect of reaction time and temperature on conversion of FUR to FFA

**Table 5.** Effect of PhP-Hf (1:1.5) dosage on transfer hydrogenation of FUR to FFA

**Fig. 1.** FT-IR spectra (A), XRD patterns (B), N<sub>2</sub> adsorption-desorption isotherms (C), and TG curves (D) of PhP-Hf (1:1.5) and HfO<sub>2</sub>

**Fig. 2.** XPS spectra of (A) Hf 4f and (B) O 1s in PhP-Hf (1:1.5) and HfO<sub>2</sub>

**Fig. 3.** HR-TEM images of (A) PhP-Hf (1:1.5) and (B) HfO<sub>2</sub>

**Fig. 4.** STEM-HAADF images (a & b), and (c) Hf, (d) C, (e) O & (f) P elemental mappings of PhP-Hf (1:1.5)

**Fig. 5.** NH<sub>3</sub>- and CO<sub>2</sub>-TPD patterns of different PhP-Hf catalysts

**Fig. 6.** XPS spectra of (A) Hf 4f and (B) O 1s in different PhP-Hf catalysts

**Fig. 7.** Possible mechanism for transfer hydrogenation of FUR to FFA catalyzed by PhP-Hf (1:1.5)

**Fig. 8.** (A) Kinetic profiles and (B) Arrhenius plot of PhP-Hf (1:1.5)-catalyzed conversion of FUR to FFA; reaction conditions: 96 mg FUR (1 mmol), 0.05 g PhP-Hf (1:1.5), and 5 mL 2-propanol

**Fig. 9.** Recycling study of PhP-Hf (1:1.5) in transfer hydrogenation of FUR to FFA; reaction conditions: 96 mg FUR (1 mmol), 0.05 g PhP-Hf(1:1.5), 5 mL 2-propanol, 120 °C for 2 h

**Fig. 10.** FT-IR spectra of fresh and recovered (after 5 cycles) PhP-Hf (1:1.5) hybrids

**Table 1.** Textural and acid-base properties of HfO<sub>2</sub> and PhP-Hf (1:1.5)

Catalyst	S <sub>BET</sub> (m <sup>2</sup> /g)	V <sub>pore</sub> (cm <sup>3</sup> /g)	D <sub>mean</sub> (nm)	Basicity (mmol/g) <sup>[a]</sup>	Acidity (mmol/g) <sup>[a]</sup>	Acid/base ratio
HfO <sub>2</sub>	23	0.17	28.9	0.24	0.16	0.67
PhP-Hf (1:1.5)	214	0.21	3.4	0.32	0.27	0.84
PhP-Hf (1:1.5) <sup>[b]</sup>	203	0.19	3.6	0.35	0.25	0.71

<sup>[a]</sup> Basicity and acidity were determined by CO<sub>2</sub>- and NH<sub>3</sub>-TPD, respectively

<sup>[b]</sup> Recovered PhP-Hf (1:1.5) after five consecutive cycles

S<sub>BET</sub>: BET surface area, V<sub>pore</sub>: volume of pores, D<sub>mean</sub>: average pore size

**Table 2.** Transfer hydrogenation of FUR to FFA with different catalysts

Entry	Catalyst	FFA yield (%)	FUR conv. (%)	FFA selec. (%)	Formation rate ( $\mu\text{mol g}^{-1} \text{h}^{-1}$ ) <sup>[a]</sup>
1	SiO <sub>2</sub>	0.6	19.0	2.9	60
2	NiO	3.1	8.6	36.2	310
3	MgO	0.5	3.6	15.1	50
4	CaO	1.4	1.8	75.6	140
5	Al <sub>2</sub> O <sub>3</sub>	22.3	29.9	74.5	2230
6	ZrO <sub>2</sub>	23.6	28.3	83.4	2360
7	HfO <sub>2</sub>	27.8	32.5	85.5	2780
8	PhP-Hf (1:1.5)	97.6	99.2	98.4	9760
9	NaOH	21.3	52.6	-	2130
10	PhP	<0.2	37.4	<0.5	<20
11	HfCl <sub>4</sub>	1.1	93.3	1.2	110
12	PhP-Ni (1:1.5)	7.5	17.4	43.1	750
13	PhP-Al (1:1.5)	36.9	45.2	81.6	3690
14	PhP-Zr (1:1.5)	77.6	86.8	89.4	7760

Reaction conditions: 96 mg FUR (1 mmol), 0.05 g catalyst, 5 mL 2-propanol, 120 °C for 2 h

<sup>[a]</sup> FFA formation rate is defined as (mol of formed FFA) / (catalyst amount × time)

**Table 3.** Effect of different P/Hf ratios on transfer hydrogenation of FUR to FFA

Catalyst	P/Hf ratio <sup>[a]</sup>	FFA yield (%)	FUR conv. (%)	FFA selec. (%)	Acid-base content (mmol/g) <sup>[b]</sup>	Acid/base site ratio	TON <sup>[c]</sup>
PhP-Hf (2:1)	2.53	46.8	50.8	92.2	0.44	0.82	23.1
PhP-Hf (1.5:1)	1.99	62.5	66.1	94.5	0.49	0.82	26.7
PhP-Hf (1:1)	1.45	85.6	88.1	97.2	0.55	0.83	32.0
PhP-Hf (1:1.5)	1.07	97.6	99.2	98.4	0.59	0.84	33.6
PhP-Hf (1:2)	0.80	97.3	99.8	97.5	0.65	0.87	30.7

Reaction conditions: 96 mg FUR (1 mmol), 0.05 g catalyst, 5 mL 2-propanol, 120 for 2 h

<sup>[a]</sup> Contents of P and Hf were obtained by XPS analyses

<sup>[b]</sup> Total contents of acid and base sites were determined by NH<sub>3</sub>- and CO<sub>2</sub>-TPD

<sup>[c]</sup> TON (turnover number) = (mole of converted FUR) / (mole of acid-base sites)

**Table 4.** Effect of reaction time and temperature on conversion of FUR to FFA

Temp. (°C)	Time (h)	FFA yield (%)	FUR conv. (%)	FFA selec. (%)	TOF(h <sup>-1</sup> ) <sup>[a]</sup>
<b>80</b>	0.25	2.8	11.7	23.9	15.9
	0.5	6.3	15.7	40.1	10.6
	1	15.7	25.3	62.1	8.6
	1.5	23.7	34.3	69.1	7.8
	2	37.3	48.1	77.5	8.2
	4	55.5	65.6	84.5	5.6
	6	68.4	79.3	86.3	4.5
	8	76.1	86.7	87.8	3.7
<b>100</b>	10	81.5	90.3	90.3	3.1
	0.25	6.5	11.5	56.5	15.6
	0.5	18.9	30.7	61.6	20.8
	1	38.7	51.9	74.6	17.6
	1.5	60.2	70.2	85.8	15.9
	2	69.3	75.2	92.2	12.7
	4	78.6	83.3	94.4	7.1
	6	87.9	92.4	95.1	5.2
<b>120</b>	0.25	15.4	23.7	65.0	32.1
	0.5	52.5	65.1	80.6	44.1
	1	74.8	86.5	86.5	29.3
	1.5	86.2	94.5	91.2	21.4
	2	97.6	99.2	98.4	16.8
	4	98.3	99.7	98.6	8.4
	6	99.9	100	99.9	5.6
<b>140</b>	0.25	43.9	50.5	86.9	68.5
	0.5	63.6	71.2	89.3	48.3
	1	84.3	92.3	91.3	31.3
	1.5	90.9	98.6	92.2	22.3
	2	98.3	99.8	98.5	16.9
	4	96.5	100	96.5	8.5
	6	95.2	100	95.2	5.6

Reaction conditions: 96 mg FUR (1 mmol), 0.05 g PhP-Hf (1:1.5), 5 mL 2-propanol

<sup>[a]</sup> TOF (turnover frequency) = (mole of converted FUR) / [(mole of acid-base sites) × time]

**Table 5.** Effect of PhP-Hf (1:1.5) dosage on transfer hydrogenation of FUR to FFA

Entry	FUR/catalyst mass ratio	FFA yield (%)	FUR conv. (%)	FFA selec. (%)	TON <sup>[a]</sup>
1	0	-	<1.0	-	-
2	8.0	40.7	42.6	95.5	60.2
3	4.0	64.3	66.2	97.1	46.8
4	1.9	97.6	99.2	98.4	33.6
5	1.3	98.5	99.7	98.7	23.5
6	1.0	99.2	100	99.2	17.7

Reaction conditions: 96 mg FUR (1 mmol), 5 mL 2-propanol, 120 °C for 2 h

<sup>[a]</sup> TON (turnover number) = (mole of converted FUR) / (mole of acid-base sites)

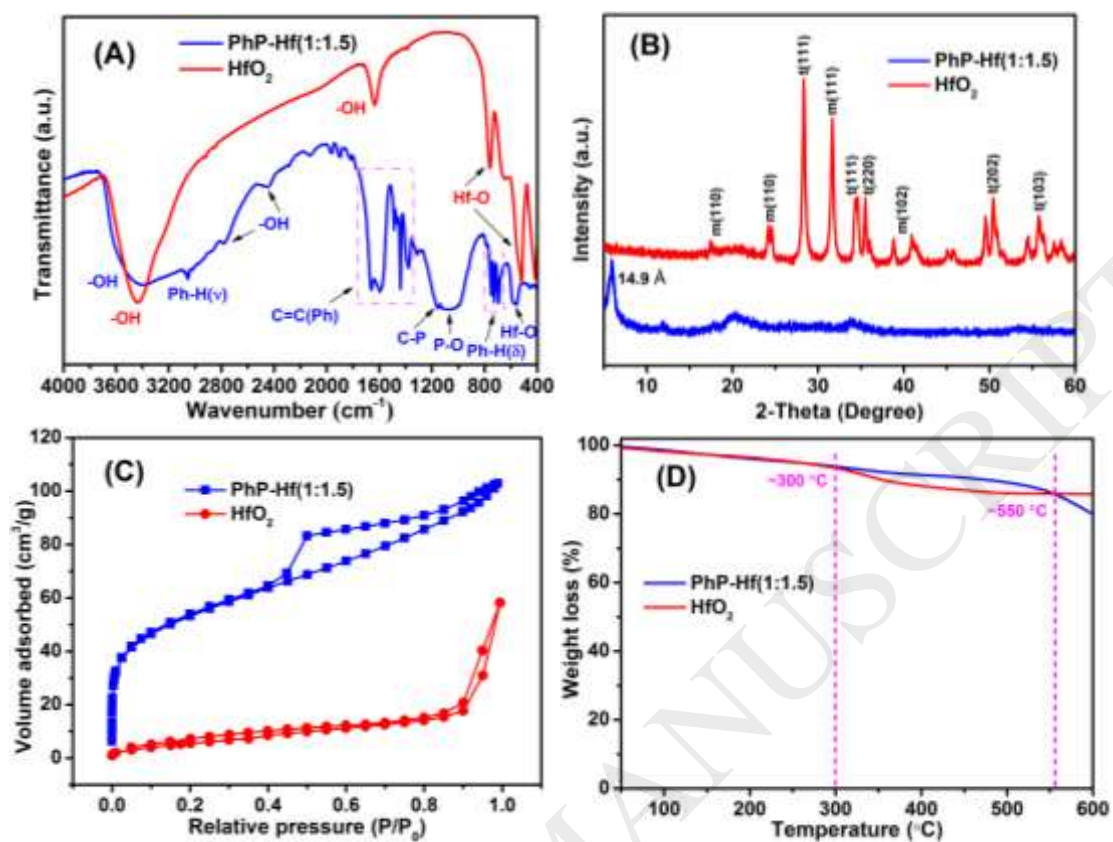


Fig. 1

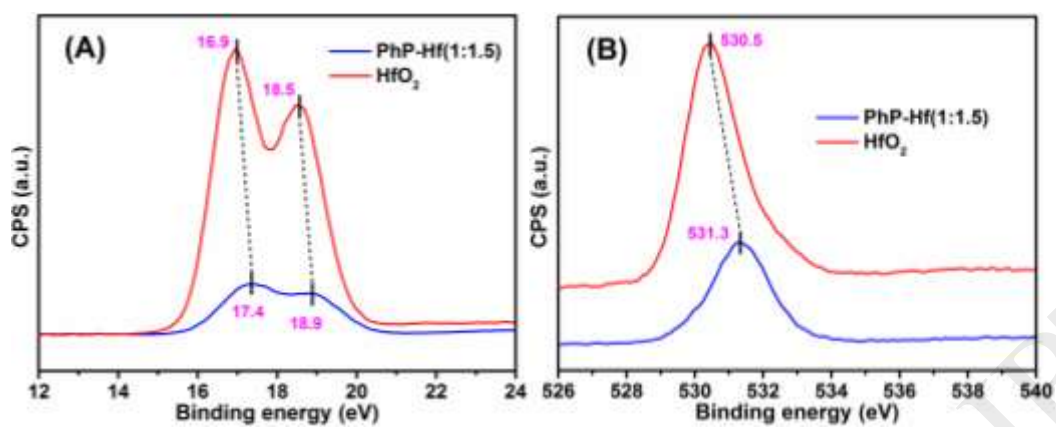
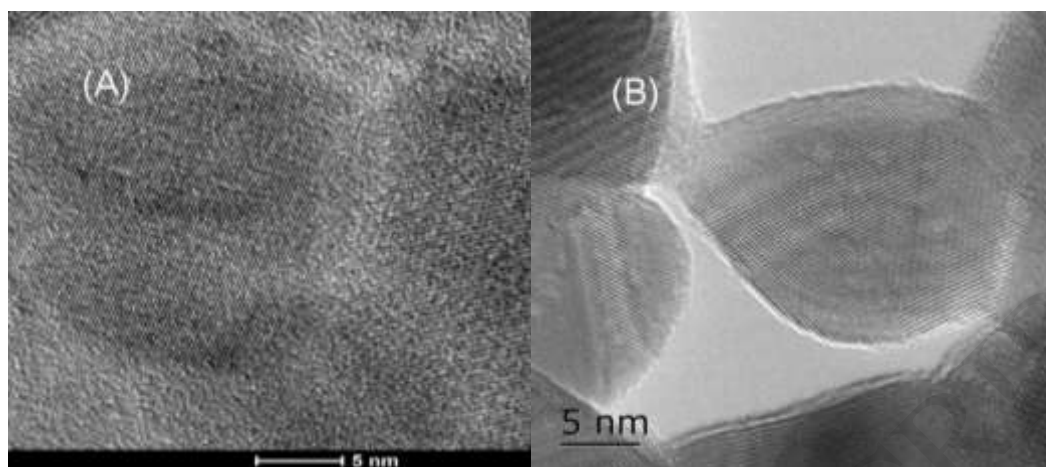
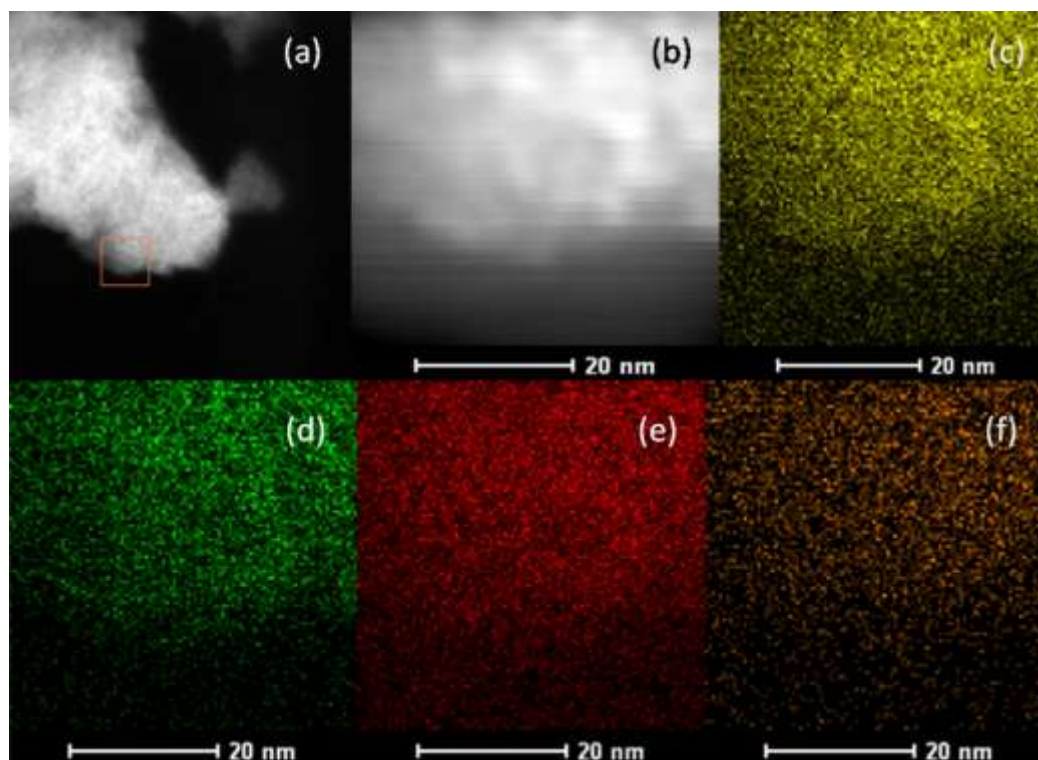


Fig. 2



**Fig. 3**

**Fig. 4**

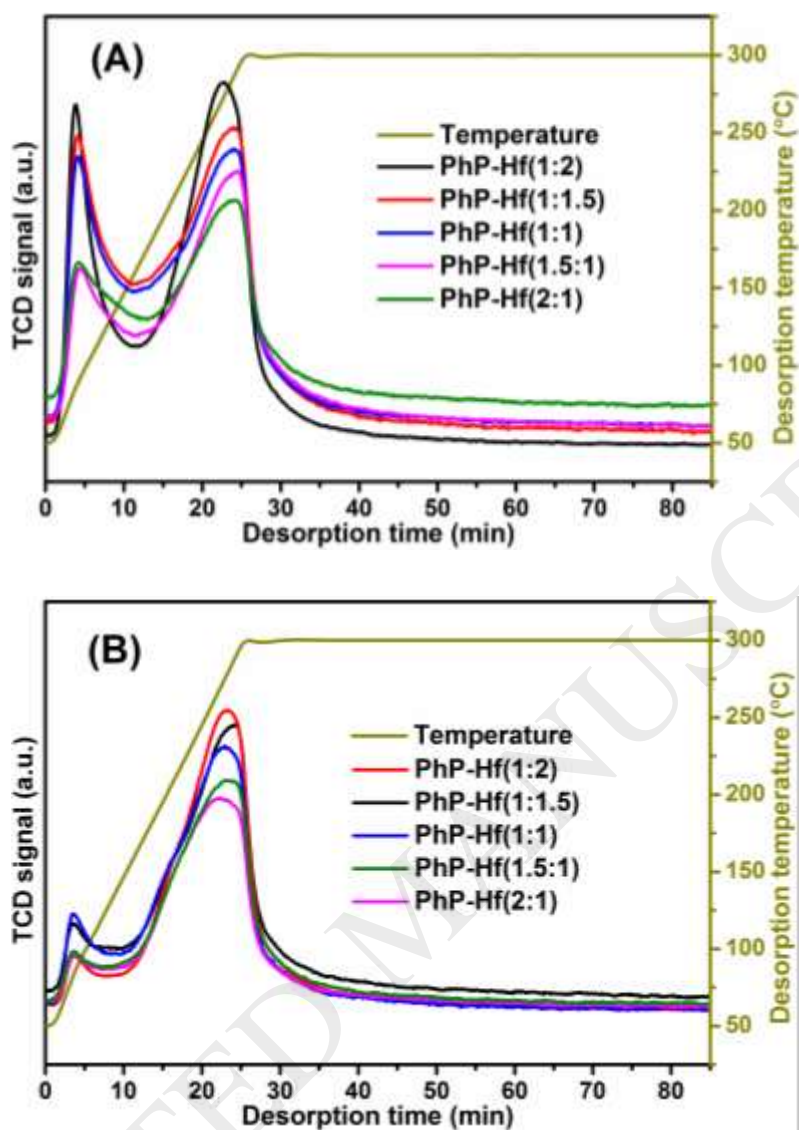


Fig. 5

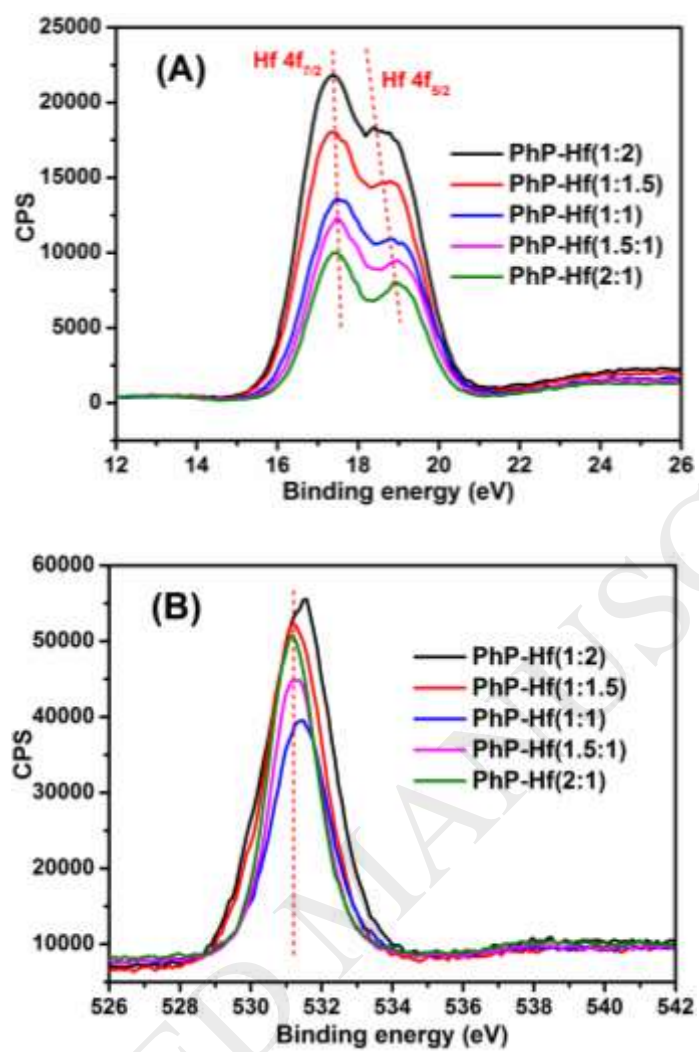


Fig. 6

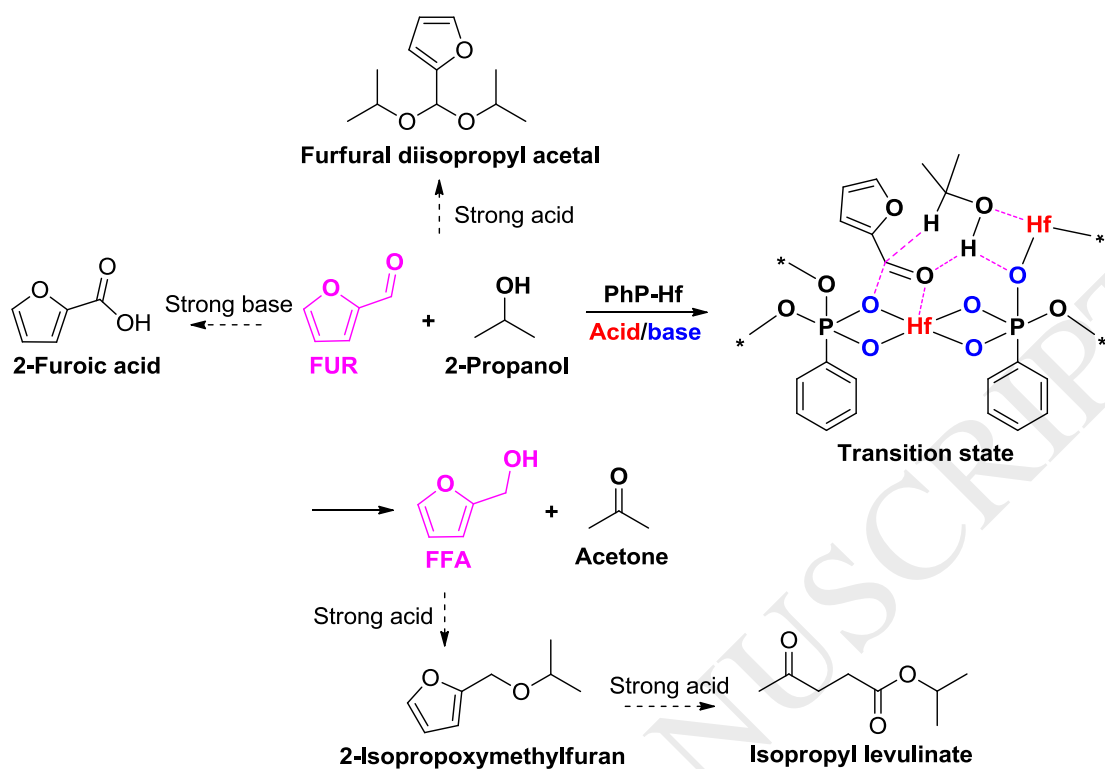


Fig. 7

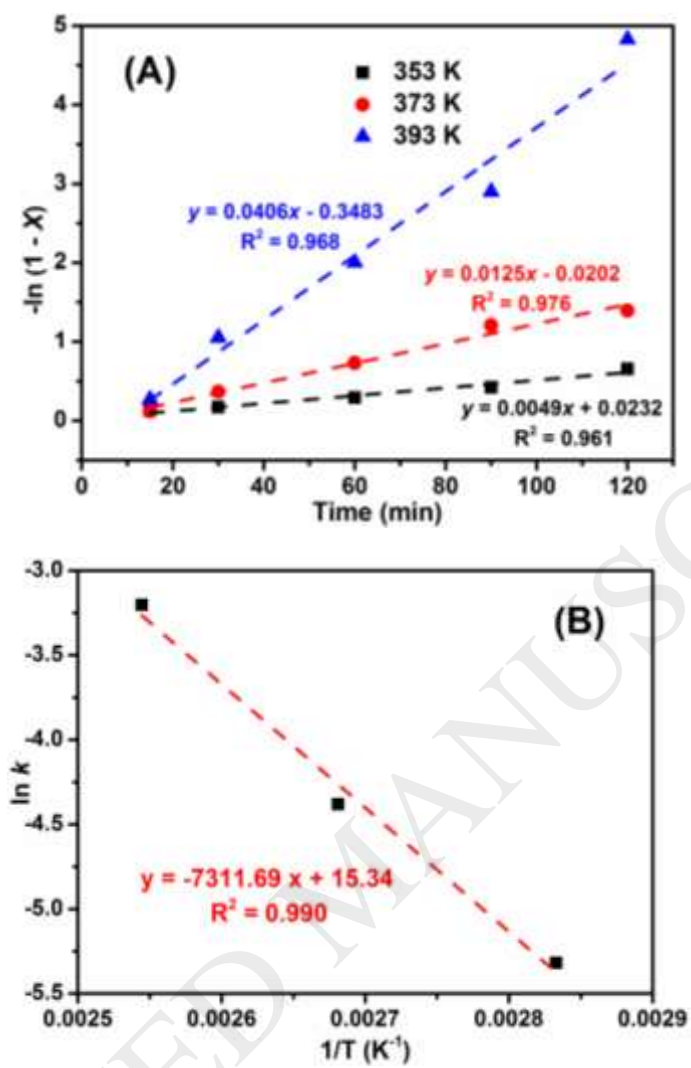


Fig. 8

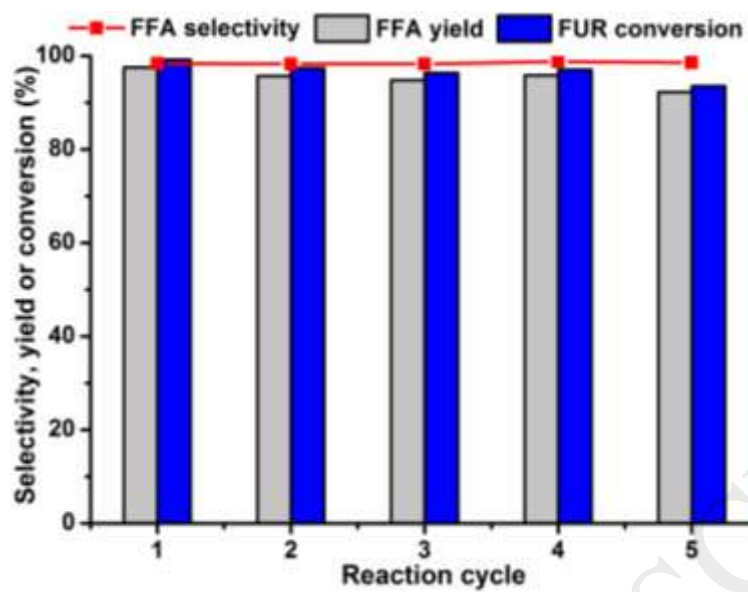
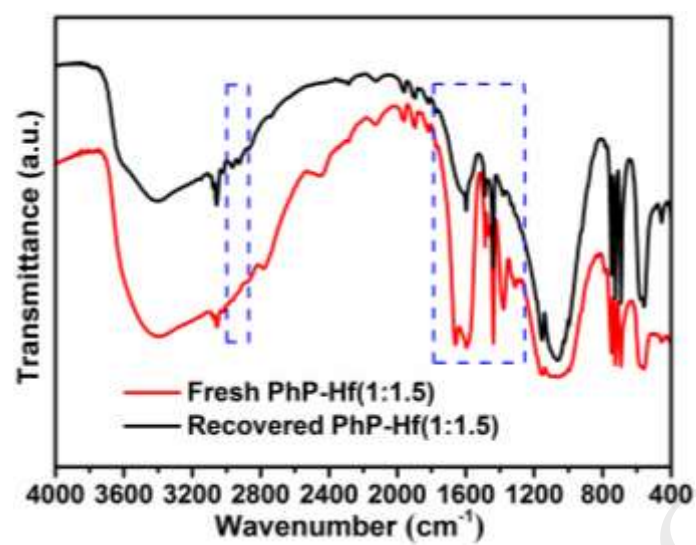


Fig. 9

**Fig. 10**